Mechatronics 49 (2018) 177–186

Contents lists available at ScienceDirect

Mechatronics

journal homepage: www.elsevier.com/locate/mechatronics

A Dual-cable Hand Exoskeleton System for Virtual Reality☆

Yeongyu Park, Inseong Jo, Jeongsoo Lee, Joonbum Bae*

Department of Mechanical Engineering, UNIST, Ulsan, Republic of Korea

ARTICLE INFO

Keywords:
Wearable system
Hand exoskeleton
Force feedback
Haptic interface
Virtual reality

ABSTRACT

In this paper, a hand exoskeleton system for virtual reality is proposed. As a virtual reality interface for the hand, a wearable system should be able to measure the finger joint angles and apply force feedback to the fingers at the same time with a simple and light structure. In the proposed system, two different cable mechanisms are applied to achieve such requirements; three finger joint angles in the direction of the flexion/extension (F/E) motion are measured by a tendon-inspired cable mechanism and another cable is used for force feedback to the finger for one degree of freedom (DOF) actuation per finger. As two different types of cables are used, the system is termed a dual-cable hand exoskeleton system. Using the measured finger joint angles and motor current, the cable-driven actuation system applies the desired force to the fingers. That is, when the desired force is zero, the motor position is controlled to follow the finger posture while maintaining the appropriate cable slack; when the desired force needs to be applied, the motor current is controlled to generate the desired force. To achieve a smooth transition between the two control strategies, the control inputs were linearly integrated; and the desired motor position was generated to prevent a sudden motor rotation. A prototype of the proposed system was manufactured with a weight of 320g, a volume of $13 \times 23 \times 8cm^3$, maximum force up to $5\,N$. The proposed control algorithms were verified by experiments with virtual reality applications.

1. Introduction

Recently, virtual reality technologies such as head mounted displays (HMDs) or wearable haptic devices have been actively investigated [4–12,14,16–18,21,24,31]. However, current virtual reality technologies mainly focus on delivering visual information, such as HMDs. Visualization of the virtual space is one of the fundamental aspects of virtual reality, but force feedback from virtual objects is also essential to achieve vivid interactions in virtual reality. To date, force delivering systems have been investigated, yet there are few systems that satisfy the requirements of force-feedback devices for virtual reality applications, i.e., mobility, motion measurement, accurate force feedback, etc.

Systems with various mechanisms have been designed to satisfy those requirements. The grounded device is fixed and applies the force from the ground (or a desk, wall, or ceiling) [29]. Many products have been commercialized, and various end effectors such as a pen, scissors, and a soft ball are used depending on the purpose of the system [6,8]. Mouse type grounded device has also been developed using MR brake and serial linkage in Fig. 1a [17]. Since the systems are fixed to the ground, they can precisely measure the position of the end effector and transmit the force accurately. However, it is difficult for the user to move around freely due to its limited workspace.

In contrast, there are ungrounded devices in which the reaction force from the user is applied to other body parts of the user, far from the area of the desired force feedback [29]. Usually, ungrounded devices are wearable, exoskeleton type devices and have improved mobility compared to the grounded devices. Wearable systems have been developed by applying various actuators and mechanisms. Koyama *et al.* implemented a passive force feedback system using a spring-coupled clutch [18]. In Fig. 1b, Tadano *et al.* used a pneumatic actuator as a power source and pulley system that can flex the finger joint by changing the pressure in the cylinder [31]. Generally, pneumatic systems can generate more power than electric actuators, but have lower mobility compared with other actuators (e.g., electric motors) due to the additional components (e.g., pumps). Most wearable systems instead use electric motors as actuators. Among them, systems using linkage mechanisms have been developed. Ho *et al.* and Iqbal *et al.* in Figs. 1c and d developed systems using serial linkage mechanism that can generate a grasp motion [11,14]. Systems where the ground of the actuator is applied to parts of the body other than the back of the hand have also been developed. In Fig. 1e, Frisoli *et al.* used an actuator positioned on the wrist and a linkage system connecting the wrist to the fingertip [7].

Unlike the linkage type mechanism, many systems have applied

☆ This paper was recommended for publication by Associate Editor Prof Michael Gauthier.

* Corresponding author.
E-mail addresses: ygpark@unist.ac.kr (Y. Park), isjo@unist.ac.kr (I. Jo), galanthus@unist.ac.kr (J. Lee), jbbae@unist.ac.kr (J. Bae).

https://doi.org/10.1016/j.mechatronics.2017.12.008
Received 2 April 2017; Received in revised form 30 November 2017; Accepted 24 December 2017
Available online 06 January 2018

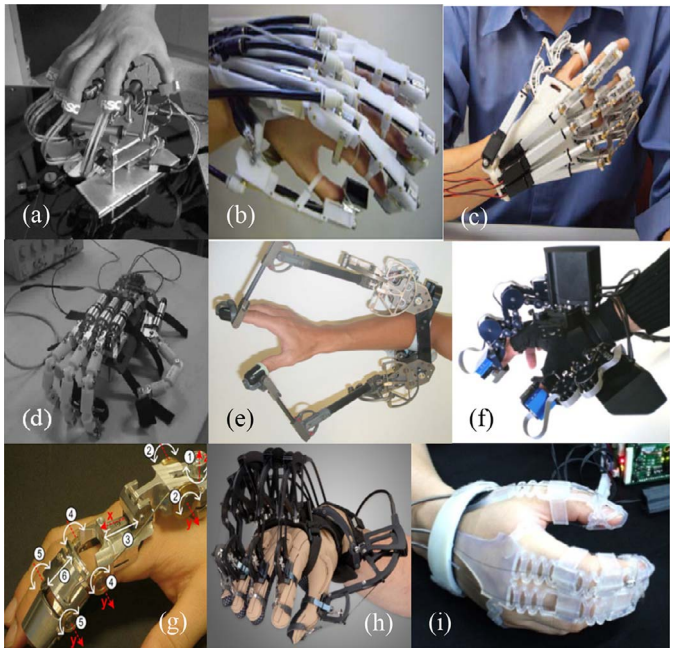

Fig. 1. Previously developed force feedback systems for the hand [4,5,7,11,14,16,17,21,31].

cable driven mechanisms. In Figs. 1f and g, Marco *et al.* and Chiri *et al.* developed a system that employs a cable pulley around the finger joints [4,21]. The Cybergrasp is commercialized product, which was developed to pull the cable connected to the fingertip to transmit a normal directional force without rotating the finger joint using a cable pulley in Fig. 1h [5]. Kang *et al.* developed a polymer-based wearable system with a wire path parallel to the fingers in Fig. 1i [16]. By adjusting the cable length in the wire path, the user can perform one degree of freedom (DOF) grasp motion.

A variety of hand exoskeleton systems have been developed using various types of actuators and mechanisms. However, most systems have a complex and bulky structures to permit various finger motion, do not measure finger motion and transmit force at the same time. In this paper, a wearable system for virtual reality applications is proposed, which uses cable-driven mechanisms to enable measurement of finger motion as well as force transmission. The main characteristics of the proposed system are as follows:

1) Two separate cable mechanisms for simultaneously realizing finger motion measurement and force feedback, and suitable structure design,
2) A non-contact null-force control by maintaining cable slack, and
3) Force control by motor current and smooth transition controller between two different control strategies.

The angles of the finger joints are measured using a tendon-inspired cable mechanism, and an additional cable is used for the force feedback to the fingertip. When no force is applied to the fingers, the force feedback cable follows the motion of the fingers with an appropriate amount of cable slack, so that zero impedance is applied. When force is applied to the finger, it is applied through the force transmission cable, which is generated by a current feedback electric motor. A smooth transition between the two control strategies (i.e., position and force control algorithms) is exploited to apply the desired force stably during active finger motions. A prototype of the proposed system was manufactured and its performance was verified by experiments.

The remainder of this paper is organized as follows. In Section 2, the structural characteristics of the hand and the requirements of a force feedback system for virtual reality are discussed. The design of the motion measurement, the force feedback mechanism and the wearable structure are discussed in Section 3. Control strategies that combine both position and force control algorithms are described in Section 4. The implementation of the proposed hand exoskeleton system and performance verification are presented in Section 5. General discussion of proposed methodologies are provided in Section 6. Finally, conclusions and directions for future works are given in Section 7.

2. Cosiderations of hand force feedback systems for virtual reality

2.1. Biomechanical characteristics of the hand

The hand is composed of various components, including bones, muscles and ligaments, so an understanding of the biomechanical characteristics of the hand, especially the fingers, is essential to develop a hand force feedback system for virtual reality applications.

Each finger except the thumb has three bones (proximal, middle and distal phalanges), and three joints (metacarpophalangeal (MCP), proximal interphalangeal (PIP), and distal interphalangeal (DIP) joints). The thumb has two bones (distal and proximal phalanges) and two joints (interphalangeal (IP) and MCP joints) [23]. Unlike the rest four fingers, the metacarpal phalanx of the thumb can be moved around the carpometacarpal (CMC) joint near the wrist, which allows complicated movements of the thumb. Each joint has one DOF for flexion/extension, and the MCP and CMC joints have one more DOF for adduction/abduction.

Fingers are characterized by a large workspace; the ranges of motion of the MCP, PIP, and DIP joints are about $0 \sim 100^{\circ}$, $0 \sim 105^{\circ}$, $0 \sim 85^{\circ}$, respectively [13]. The hand can apply cyclic motions with frequencies under 2 Hz with a continuous maximum force of 7 N in daily life [19,27].

Thus, a hand force feedback system should be developed considering the above-mentioned biomechanical characteristics of the fingers. However, the practical requirements of a hand force feedback system should be considered at the same time, which are based on the fact that flexion/extension (F/E) motion is dominant over abduction/adduction (A/A) motion when manipulating an object (e.g., grasping a object) and the user can control the object including its position and orientation with three fingers [26]. Further requirements of a hand force-feedback system and how the proposed system was designed to satisfy such requirements will be discussed in the next section.

2.2. Requirements of a hand force feedback system for virtual reality

Hand force feedback systems have been investigated for many purposes, including rehabilitation and virtual reality [4–8,10–12,14,16–18,21,24,31]. By analyzing the preliminary systems for virtual reality, including the biomechanical characteristics of the hand, we considered the requirements for a hand force feedback system for virtual reality applications and defined quantitative goals for the proposed system.

2.2.1. Wearability

The hand force feedback system for virtual reality should be easy to put on and take off, without requiring any assistance. Glove- or Velcro-type devices are the most popular types of wearable hand force feedback systems [4,5,7,10,11,14,16–18,21,31]. The glove-type system is simple to use; however, various sizes should be prepared for the users with different hand sizes. Velcro-type systems may be more flexible in terms of hand size, but require more time to put on than glove-type systems. In this paper, we used a glove-type exoskeleton for easy wearability.

2.2.2. Mobility

The user should be able to move freely while wearing the hand exoskeleton system. To enable the user to move freely, a hand

exoskeleton system should be light, and all the required components should be integrated into a single system. Thus, electric motors were used in this system because pneumatic or hydraulic systems require additional components (e.g., pumps), which cannot be easily integrated into a wearable device.

2.2.3. Design

Because the target users for virtual reality are the general public, rather than specific user groups, the system should be small and lightweight. Currently, the VIVE controller, which is commercialized in VR games, weighs about 200 g [12]. The system should have similar or reasonable weight when considering functionalities compared to the commercialized products.

2.2.4. Force distribution

Tensile forces should be applied in the normal direction to apply a reaction force from objects. A wearable system that could apply forces to all of the fingers and the palm would be ideal, but, this would require many actuators and sensors, making the system bulky and heavy. Considering the number of required actuators and sensors, as well as the hand size, the forces will be applied to the fingertips only in this system, because the fingertips are the most important parts of the hand in terms of the concentration of the force at the fingers [15]. To minimize the size of the system, the forces will be applied only to the thumb, index finger, and middle finger, as these three digits are dominant in manipulation of objects [1,26].

2.2.5. Finger motion measurement

To interact with virtual objects, the relative positions of the objects and fingertips should be accurately calculated. It means that the motion measurement accuracy should be less than finger position sensing resolution of the human, which is known to be about 2.5° for each finger joint [32]. In the proposed system, finger postures were calculated by a previously developed mechanism at a measurement error of less than 1° [25].

2.2.6. Force feedback

Most importantly, the hand exoskeleton system should be able to apply a desired force to the fingertips where the range of desired force is related to the type of task to be simulated. It is known that maximally 200 ~ 400 N force is applied during power grasp motion [28]. However, the purpose of the proposed system is to simulate the forces that are usually necessary in a daily life such as pinching, etc. Also, huge actuators would be required, which cannot be attached above the hand, to generate the force corresponding to the power grasp. Therefore, the required maximum force of the proposed system was set to 7 N, which is commonly applied in daily living (e.g., jar opening, tooth brushing) [27].

3. Design

As discussed in Section 2, the hand exoskeleton system for the virtual reality application should have a lightweight and a small volume. For this purpose, the proposed system uses only cables for finger motion measurement and force feedback, and designs small structure suitable for cable driven mechanisms. One of cables is stitched over the phalanx containing the joint to be measured and connected to a potentiometer on the back of the hand for finger motion measurement. The other cable connects the fingertip directly to the motor for force feedback and is always guided in the direction of F/E motion by the finger structures. Since the proposed device uses mechanisms using cables only, the finger structures are not required to be connected via a link and its only function is to guide the cables. Therefore, the finger structure is designed independently for each phalanx using structural guiding channels. As a result, the proposed device is small and light of 320 g in weight and 13 × 23 × 8cm^3 in volume, respectively, and especially the finger structure is small with a height of 2 cm.

3.1. Finger motion measurement

The fundamental mechanism to measure finger joint angles using flexible cables and potentiometers was developed in our previous work [25]. In this system, one cable is installed on the middle of the phalanx containing the finger joint to be measured, where the change in the cable length according to the finger movement is measured by a potentiometer on the back of the hand. As the finger is flexed and extended, the cable, which is tied to the middle of the phalanx of the finger, moves along with the length change of the finger joint, and the movement of the cable is measured by a potentiometer. The flexed finger angle is calculated from the length change measured by a potentiometer under the assumption that the finger joint is modeled as a circular disk. The tension of the cable is always maintained by a linear spring attached to the potentiometer. Little torque is generated as the springs with low elastic constant are used, with the result that deformation of the glove is negligible once the system is put on. Therefore, in preliminary research, the tracking error of the developed finger motion measurement system was about 1°, which is less than the position sensing resolution of the human [32]. Further details can be found in [25].

Due to the musculoskeletal structure, the DIP joint cannot move independently from the PIP joint, and it is known that the DIP joint angle is approximately 2/3 of the PIP joint angle [30]. However, this approximation may decrease the measurement accuracy since the relation of the DIP and PIP joint angles is slightly different in each individual [20]. In the proposed system, three cables and three potentiometers are used to measure three finger joint angles more accurately for each finger, as shown in Fig. 2c. The finger structures, which are attached to the finger joints, have a channel at the bottom to guide the motion measurement cables with the finger movement for accurate motion measurement.

3.2. Force feedback

The proposed system uses the motor current to control the tension of the cable, where the motor pulley is connected directly to the fingertip as shown in Figs. 2b and 2 c. Using the measured finger joint angles and currents of the motor, the proposed system can follow the motion of the fingers while applying force feedback. When the system does not apply a force (non-contact with an object), the motor is controlled to follow the finger motion with an appropriate amount of cable slack using the measured joint angles. When a force needs to be applied (in contact with an object), the motor controller is changed smoothly from position to current control, so that the exoskeleton system can apply the desired force to the fingers without a sudden impact from the motor. Details of the control strategies are discussed in the following section.

3.3. Structure of the hand exoskeleton system

Due to the cable driven mechanism, the structures of the proposed system are designed to be small and lightweight. In particular, the finger structures are made independently for each finger phalanx and only have height of 2 cm as shown in Fig. 2b. Other systems have been usually developed as linkage type system with serial or parallel mechanism with complex structures to allow enough range of motion of the fingers, therefore, the size of the structure of the fingers were large [11,14]. In the case of devices which used cable mechanism, they also have large volume because of the pulley, which is the additional structure to convert the cable tension to the force on the finger phanlanges [21]. Compared to conventional systems, the proposed system does not require links between the structures and pulleys on the joint because it transmits the normal direction of force to the fingertip through the cable. The finger structure is just designed to guide the cable so that it does not come off the fingers and fingertip. Therefore, as shown in Fig. 2b, the finger

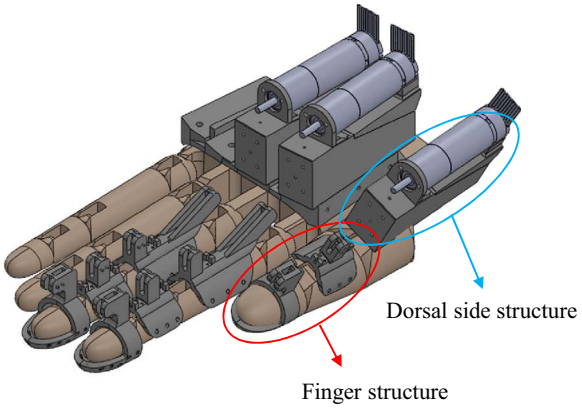

(a) Structure design of the proposed system

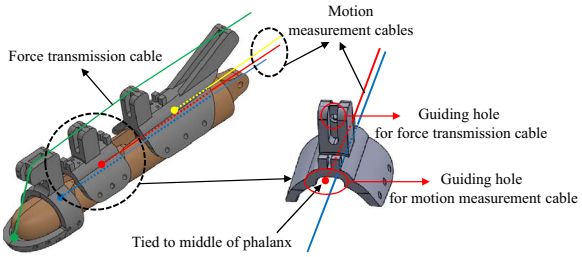

(b) Design of finger structure

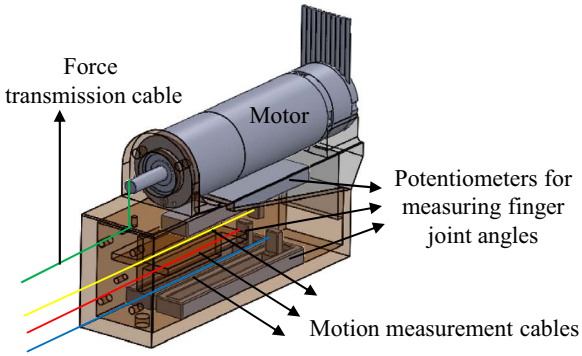

(c) Design of dorsal side structure

Fig. 2. Description of the proposed system design.

structure was designed independently for each finger phalanx and has two guiding apertures. The upper part of the structure guides the force transmission cable and the lower part guides the finger motion measurement cable. Also, the finger structures are manufactured to deliver the force efficiently. The independent structures are rigid to withstand the tension of the cable and are fixed with stitches instead of glue to fasten the structure and the glove stronger even in the deformation of the glove. However, the total volume of the system is 8 cm in height because it requires three potentiometers and one motor per finger to be located within the range of the finger width on the dorsal side of the hand for a smooth cable connection.

4. Control strategy

4.1. Position control with slack

To enable the user to move his or her finger freely, the motor should wind and unwind the force transmission cable (red line in Fig. 3) appropriately along with the finger motion. That is, the length of the force transmission cable should be calculated in terms of the angles of the finger joints.

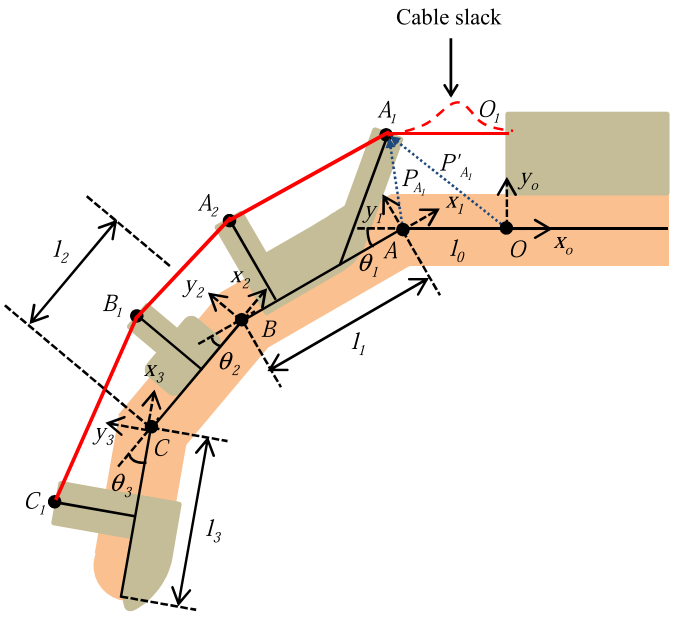

Fig. 3. Coordinates for calculating the force transmission cable length and cable slack.

As the finger flexes and extends in a plane, the required length of the force transmission cable is the sum of the distances that connect each of the holes (O_1, A_1, A_2, B_1 and C_1 in Fig. 3) of the finger structures. Thus, the length of the force transmission cable as a function of each finger joint angles is obtained by calculating the position of the finger structures and summing the linear distances between each aperture of finger structures. The required length of the force transmission cables, L, using the coordinates shown in Fig. 3 is calculated as follows:

$$L = |P'_{A_1} - P'_{O_1}| + |P'_{A_2} - P'_{A_1}| + |P'_{B_1} - P'_{A_2}| + |P'_{C_1} - P'_{B_1}| \quad (1)$$

where P'_{O_1}, P'_{A_1}, P'_{A_2}, P'_{B_1} and P'_{C_1} are the positions of O_1, A_1, A_2, B_1 and C_1 with respect to the 0^{th} frame (x_0, y_0 in Fig. 3). Each position is calculated by a transformation matrix.

$$\begin{aligned} P'_{A_1} &= T_{01} P_{A_1} \\ P'_{A_2} &= T_{01} P_{A_2} \\ P'_{B_1} &= T_{01} T_{12} P_{B_1} \\ P'_{C_1} &= T_{01} T_{12} T_{23} P_{C_1} \end{aligned} \quad (2)$$

$$T_{n-1,n} = \begin{bmatrix} \cos\theta_n & -sin\theta_n & 0 & -l_{n-1} \\ \sin\theta_n & \cos\theta_n & 0 & 0 \\ 0 & 0 & 1 & 0 \\ 0 & 0 & 0 & 1 \end{bmatrix} \quad (3)$$

where $T_{n-1,n}$ is the transformation matrix from the $(n-1)^{th}$ frame to the n^{th} frame ($n = 1, 2, 3$). P_{A_1}, P_{A_2}, P_{B_1} and P_{C_1} are the positions with respect to the coordinates on each finger phalanx, defined as $P_i = [P_{ix} \;\; P_{iy} \;\; 0 \;\; 1]^T$ where P_{ix} and P_{iy} are the x- and y- axes positions of i points. In Fig. 3, P'_{A_1} and P_{A_1} are represented as position vectors from the reference frame to the point by the blue dashed line.

The length change of the force transmission cable can be analytically calculated by (1)–(3) using the measured angles. However, analytical cable length contains many parameters such as the lengths of each finger phalanges (l_0, l_1, l_2) and the positions of the structures (A_1, A_2, B_1 and C_1), which are changed for each user or trial. In this paper, more practical method with two calibration postures to estimate the required cable length is proposed. Fig. 4 shows the calculated length by the measured data (finger phalanges length and positions of structures) and the linearly fitted length. The cable length is calculated as one finger joint (MCP, PIP and DIP joints) moves from 0° to 90°. As the length change of the force transmission cable follows a linear relationship with the joint angles, the cable length change was linearly

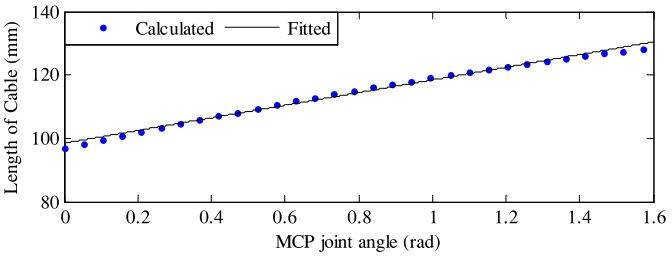

(a) Analytically calculated cable length and the linear fitting by the MCP joint angle change

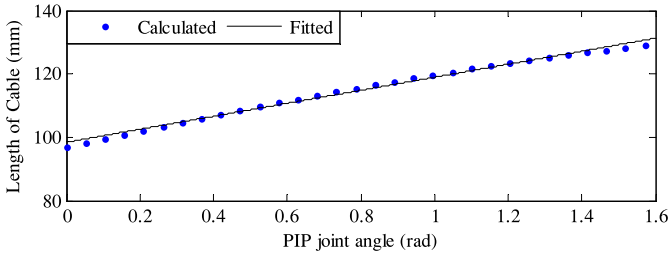

(b) Analytically calculated cable length and the linear fitting by the PIP joint angle change

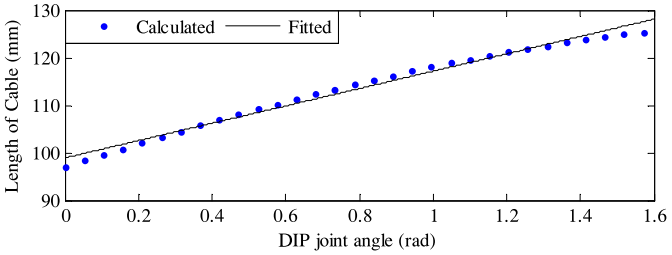

(c) Analytically calculated cable length and the linear fitting by the DIP joint angle change

Fig. 4. Required force transmission cable length in terms of finger joint angles.

fitted with respect to the joint angles; the root mean square errors (RMSEs) for the MCP, PIP and DIP joints are as small as 0.8246, 0.8298, and 1.403 (*mm*), respectively. For example, the following linear relationship was obtained for Fig. 4,

$$T_{pos} = 20.03\theta_{MCP} + 20.55\theta_{PIP} + 18.28\theta_{DIP} + \theta_{init} \quad (4)$$

where T_{pos} (rad) is the desired motor position as the joint angle changes and θ_{init} (rad) is the motor position at the full extension posture of the hand. θ_{MCP}, θ_{PIP} and θ_{DIP} are the angles of the MCP, PIP, and DIP joints, respectively.

However, the proposed system cannot unwind and wind the force transmission cable along the finger motion when using (4) for motor position control. This is because the finger joint should move first in order to change the length of force transmission cable, but the finger joint cannot move in advance when the cable tension is tightly maintained. For this reason, we allowed for slack in the cable during position control, i.e., the motor position is controlled to follow the finger movement while maintaining the desired amount of slack represented by the red dashed line in Fig. 3. In addition, a certain amount of cable slack yields no resistive forces on the fingers, which allows the finger to move freely. In the proposed system, the length of cable slack is set to be 4 mm, which can maintain zero force even with uncertainty of the interactions from the user. The actually applied force transmission cable length along the finger motion is as follows:

$$T_{pos} = 20.03\theta_{MCP} + 20.55\theta_{PIP} + 18.28\theta_{DIP} + \theta_{init} + \theta_{slack} \quad (5)$$

where all parameters are the same as (4) and θ_{slack} (rad) is the constant cable slack.

In the actual application, the parameters of the linear fitting were obtained experimentally by two calibration postures (i.e., full extension and flexion) for each trial. To conclude, the desired motor position is calculated by a linear function from each finger joint angles with a certain amount of slack. The motor tracks the trajectory using a proportional integral derivative (PID) controller, in which the controller gains were tuned heuristically.

4.2. Force control by current feedback

For force control, it is generally recommended to install a force sensor to measure the interaction force between the user and the force feedback system. However, commercial force/torque sensors are too large and heavy for a small system such as a hand exoskeleton. It is well known that the torque generated by an electric motor is proportional to the current [3], thus the torque can be calculated by measuring the current. However, the relationship between the torque and current may be nonlinear due to the nonlinearities introduced by the gear box. But, because the gear ratio of this system was small as 28: 1, the relationship may be approximated to be linear. Thus, the relationship between the force and current was fitted using the linear function in Fig. 5. Using this function, the applied force was controlled using current feedback with a manually tuned PI controller. Considering the maximum force of the human finger about 7 N [27], the motor is turned off when the motor current (0.3 *A*) corresponding to the maximum force (5 *N*) of the proposed device is exceeded.

4.3. Transition controller

For virtual reality applications, the force-feedback system needs to apply various magnitudes of force to the user. Zero force can be applied as the motor winds and unwinds the force transmission cable following the user's motion, which was achieved by the position control with a slack, as discussed in Section 4.1. When the system applies the force, the motor changes the control strategy from position to force control, as discussed in Section 4.2. Then, the switching between position and force control should be smooth as a rapid change of the control modes may cause undesired vibration or sudden rotation of the motor. In the proposed system, we considered smooth transition methods for the control inputs and the desired motor position.

First, a smooth transition between the position and force control schemes was achieved by integrating the control inputs from two control strategies using the linear weighting function in Fig. 6. For example, when the motor changes the control from position to force (e.g., when the finger touches a virtual object), a decreasing proportion of position control and an increasing proportion of current control are integrated so that the motor changes the control mode smoothly, as:

$$u = \left(\frac{d-x}{d}\right)u_p + \left(\frac{x}{d}\right)u_f \quad (6)$$

where u is the total control input in transition range, u_p and u_f are the control inputs of position and force controller, respectively. d is the

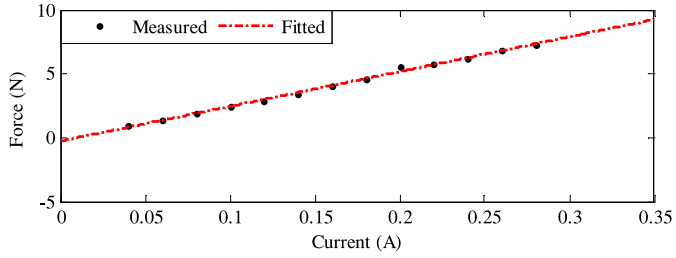

Fig. 5. Relationship between the motor current and force.

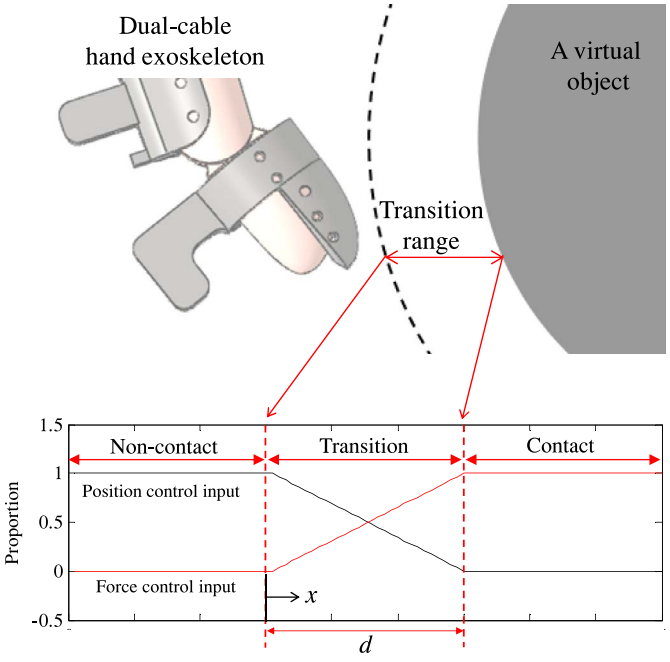

Fig. 6. Transition mechanism between position and force control.

length of transition range and x is the position in the transition range shown in Fig. 6. Although Fig. 6 shows only the transition from position to force controller, the same transition scheme is applied when the controller is changed from force to position mode.

Second, the desired motor position is generated in the transition as shown in Fig. 7a when the motor changes the control from force to position. This scheme is necessary because the motor in the force controller is tightly wound to apply the force, but the cable has a slack in the position controller to enable the free finger motion.

A detailed finger motion is shown at the top of Fig. 7a: the finger is flexed to touch a virtual object and turned back. In this case, the finger is flexed inside the virtual object to show two different transition cases (first and second transitions at the bottom of Fig. 7a). When the finger flexes to touch the virtual object (first transition range in Fig. 7a), the motor winds the cable by the transition scheme in Fig. 6 and (6). Therefore, there is no sudden motor rotation in the transition during the touching an object. However, when the finger is detached from the object, the cable slack is added to the desired motor position, which may cause sudden motor rotation. Thus, the transition was achieved by integrating the desired motor trajectory of the position controller, M_{pos} (the motor position along the finger motion with a slack (i.e., T_{pos} + cable slack)), and M_{for} (the motor position when the finger is just detached from the object, i.e., the boundary of the virtual object) as below:

$$M_{trans} = \left(\frac{d-x}{d}\right)M_{for} + \left(\frac{x}{d}\right)M_{pos} \tag{7}$$

where M_{trans} is the desired motor position in the transition range, M_{pos} and M_{for} are represented as black and blue dotted lines in Fig. 7b, respectively; d and x are same as in Fig. 6. The desired motor position is calculated by the two motor positions with different proportions. For example, at the second point in Fig. 7b where x is $d/5$, the proportion of M_{for} and M_{pos} is 4/5 and 1/5, respectively.

4.4. Overall controller

The overall control algorithm for the dual-cable hand exoskeleton system is shown in Fig. 8. The position of a virtual object is assumed to be known by a virtual reality program. The fingertip positions are measured using the motion measurement cables and potentiometers (in

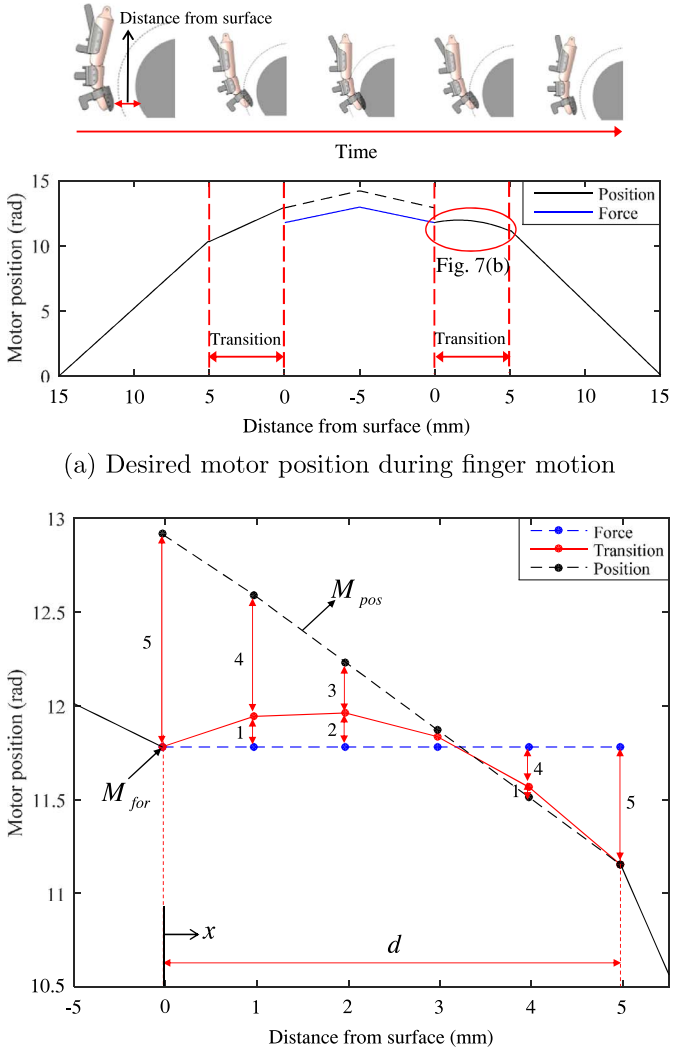

Fig. 7. Transition mechanism in terms of motor position.

this paper, only finger motion was measured, but the position and rotation of the hand itself are considered as known, which can be measured later by the infrared camera based motion capture system). According to the relationship between the position of the fingertip and the position of the virtual object (e.g., non-contact, touching the object and detaching from the object), the transition controller of (7) sets the desired position (M_{trans}) for position controller. The distance between the fingertip and the object position generates an interaction force using a mechanical model of the virtual object (this is not discussed in detail here, although a simple algorithm will be described in Section 5). Based on the desired values (M_{trans}, f_d) of the two controllers, the position and force controllers calculate the control inputs (u_p, u_f) to be applied to the motor, respectively. The transition controller of (6) controls the actual motor by distributing the appropriate proportion to the respective control inputs according to the distance between the human hand and the virtual object.

The controller of the proposed device controls one actuator based on one fingertip position and the information of the virtual object. Therefore, the proposed system can interact with virtual objects using three fingers at the same time, but each actuator is controlled independently by one controller to the desired force and position to each finger.

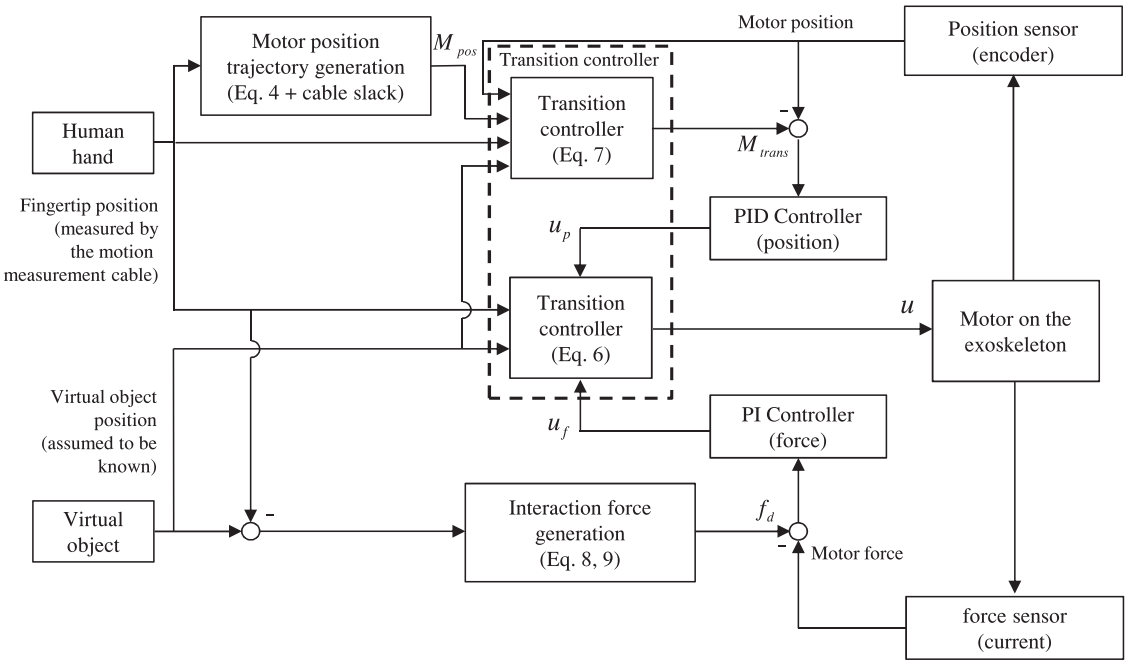

Fig. 8. Control block diagram of the proposed controller.

4.5. Experimental verification

Before applying the proposed control strategy to the hand exoskeleton system, the performance of the motor control was verified by the simple experimental setup. A motor and one potentiometer were connected via a force transmission cable, while three potentiometers were used in the actual system. As the user changed the position of the potentiometer, the motor tracked the generated trajectory to follow the movement of the potentiometer, while maintaining the desired amount of slack; or the desired force was applied via the cable.

Fig. 9 shows the results of the position controller experiment. Fig. 9a shows the calculated and measured angular positions of the motor, including the slack, and Fig. 9b shows measured slack. The position controller tracked to the desired position accurately, while maintaining the slack. The cable slack was set to 4 mm, and it was maintained with a RMSE of 0.2335 mm. By maintaining this slack, the user did not experience any resistive forces during the free motion of potentiometer, which can be interpreted as a finger movement.

Finally, the overall controller was implemented, and the results are shown in Fig. 10. The motor followed the potentiometer movement without any sudden rotations during transitions as shown in Fig. 10a. Furthermore, the cable slack was maintained at 4 mm shown in Fig. 10c. During the force control, a constant force of 2 N was applied. As shown in Fig. 10b, the desired force was generated accurately. Although the force measured using the motor current indicates that some force was exerted during position control, the user could not feel this force due to the cable slack.

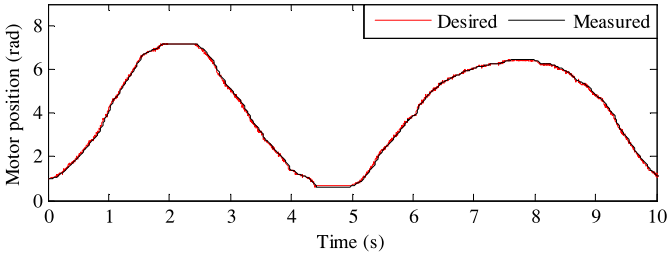

(a) Motor position during position control

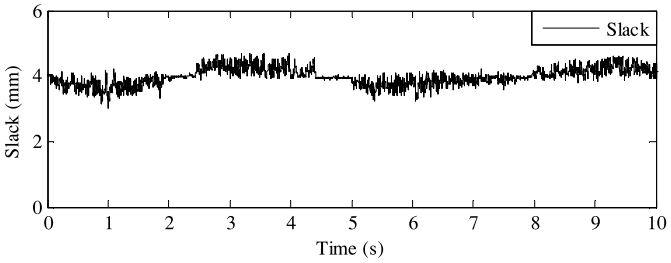

(b) Slack of the cable

Fig. 9. Performance verification of position control with a slack.

5. Implementation and applications

5.1. Implementation

Fig. 11a shows the prototype of the hand exoskeleton system. Three motors (DCX 16S, Maxon [22]) were used considering the maximum torque and speed. Given the restricted space and the capabilities of the hand, only three actuators were applied to the thumb, index finger and middle finger. The motors and potentiometers were located on the dorsal side of the hand and were connected to the fingers via cables. The total weight of the system was 320 g, and the dimensions were $13 \times 23 \times 8$ cm^3.

5.2. Applications to virtual reality

Two experiments were carried out as virtual reality applications; the first one was to provide constant force from a hard object and the second one was to generate linear force from a soft object modeled as a virtual spring as shown in Figs. 11b and c, respectively. The virtual object and hand were displayed on the monitor to provide visual feedback to the user as shown in Fig. 11d. In the experiments, the user recognized the virtual sphere using three fingers. However, as described in Section 4.4, since the three actuators are independently controlled through one controller, the same experimental results would be obtained for each actuator. Hence, the experimental results were showed

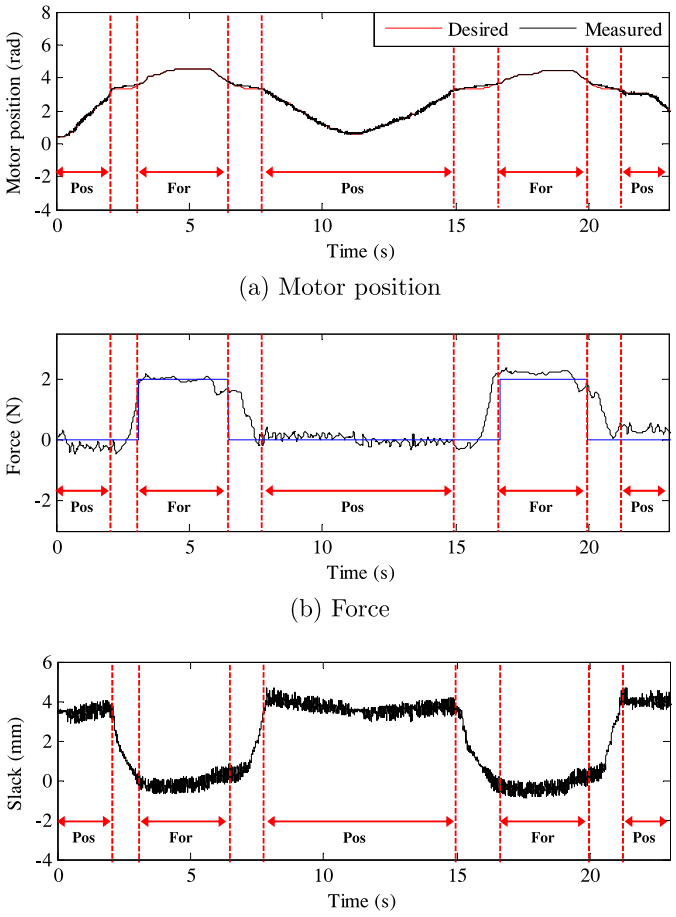

Fig. 10. Performance verification of the proposed control strategy.

only the results obtained from one actuator.

The exoskeleton system was set to generate a constant force when in contact with a virtual hard ball, when the motion occurred as follows.

$$f_{des} = \begin{cases} 0, & l_x \geq r \\ f_{const}, & l_x < r \end{cases} \quad (8)$$

where l_x is the length from the center of the virtual object to the fingertip, r is the radius of a virtual sphere and f_{const} is the constant force. The desired force was set to be zero in free space and became constant when the fingertip touched the surface of the virtual sphere. In this experiment, f_{const} was set to 2 N, and r was set to be 50 mm. As shown in Fig. 12a and 12 b, the hand exoskeleton system generated a 2 N force when contact with the virtual ball occurred, that is, when the distance to the origin of the virtual ball was 50 mm, the same as the radius of the virtual object. When the fingers were not in contact with the virtual ball, the user could not feel any resistive force due to the cable slack even though Fig. 12b shows a little force during position control (i.e., non-contact).

The second experiment was designed to investigate interactions with a soft object. The reaction force from various objects has been modeled in several ways, considering the mechanical characteristics of the object [2], but the reaction force was simply modeled as a linear spring in this experiment, which generates a proportional force to the deflection of the virtual object as follows:

$$f_{des} = \begin{cases} 0, & l_x \geq r \\ k_{vir}(r - l_x), & l_x < r \end{cases} \quad (9)$$

where k_{vir} is the virtual spring constant. The force was applied linearly

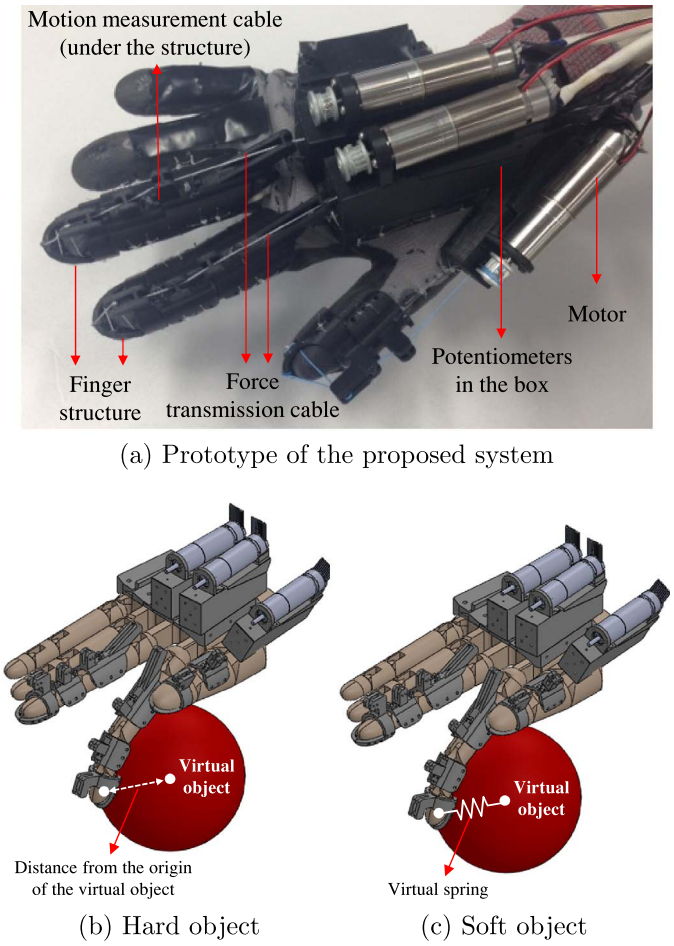

Fig. 11. Prototype and experiments with a virtual object.

in terms of deflection of the virtual sphere by Hooke's law.

The two main functions of the hand exoskeleton system (i.e., measuring the finger joint angles and applying forces to the fingertips) were exploited to apply the desired force during movement of the fingers. Three spring constants were investigated: 0.3, 0.5, and 0.8 N/cm as shown in Fig. 12c. As the finger moved, the deflection of the virtual object was calculated from the measured fingertip positions, and the desired force was determined based on the spring constant. Fig. 12c shows that the proposed system could generate the desired force accurately with respect to the finger joint angles measured in real time.

6. Discussions

The proposed system introduced new methodologies and verified their performances experimentally; two separate cable mechanisms for finger motion measurement and force feedback, and force/position

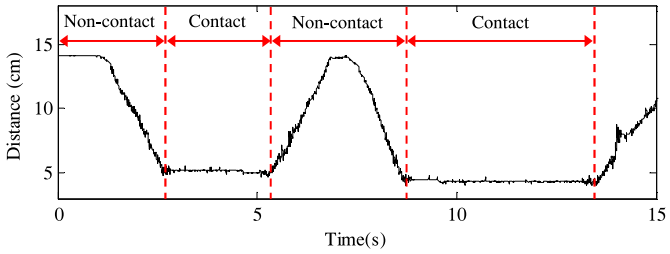

(a) Distance from the origin of the virtual object

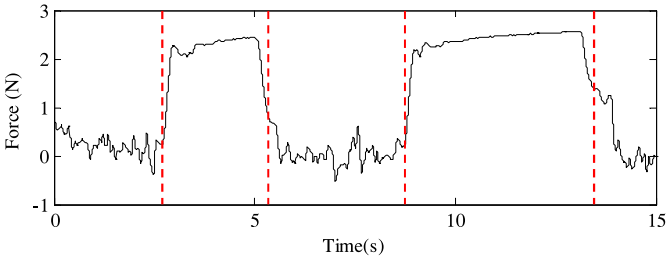

(b) Applied force for realizing a hard object

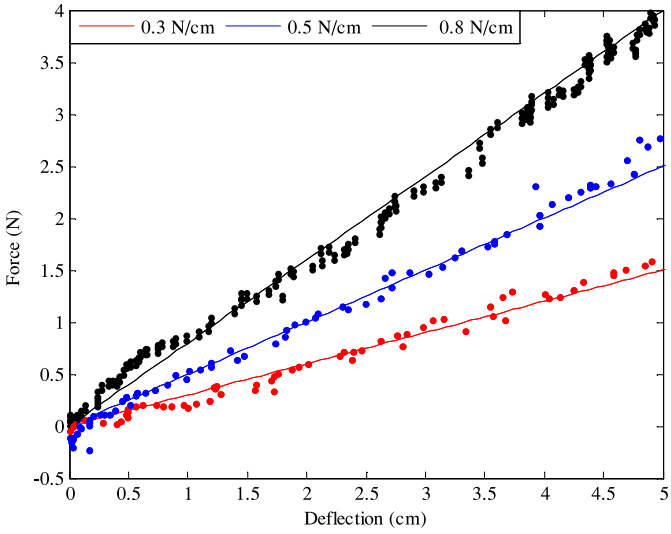

(c) Interaction with soft objects of different stiffness

Fig. 12. Interaction with a hard and soft object.

switching control. However, there would be alternatives to the proposed methodologies. In this section, general discussions of the proposed methodologies are provided compared with the alternatives.

In the proposed system, three cables were used to measure MCP, PIP and DIP joint angles and the other cable was used for force feedback. The cable for force feedback could be used for finger motion measurement because the cable length change was measured by the motor encoder. However, the reason why we used separate cables to measure the finger joint angles is that we need to measure three joint angles (MCP, PIP, and DIP joints), but only one cable is used for force feedback. If we use one force feedback cable to measure joint angles, we cannot distinguish, for example, MCP joint movement and PIP joint movement. Thus, we used the separate three cables to measure the three joint angles independently. Also, the resistive forces derived by the measurement cables are very small as maximally 0.1 N due to the use of a spring with a low elastic modulus of 0.0087 N/mm, thus it does not interfere natural movement of the fingers.

For precise force feedback, the proposed system used position/force switching control; the cable was controlled by position control with a slack in non-contact case and current control in contact case. The alternative would be to use the actuation mechanism only with current control; the cable always maintains the tension and behaves as a spring with very low stiffness by null current control in non-contact case and the same current control used in the proposed system is applied in contact case. But it is very difficult to compensate the dynamic effect such as rotor inertia with maintaining the cable tension at all time. If we allow the cable slack, the haptic transparency can be easily guaranteed when zero force is required.

7. Conclusions and future works

In this paper, a hand exoskeleton system was developed, which measures finger motion and applies the desired force concurrently, using light weight and compact structures. Finger structures were manufactured independently to permit passive finger motion and has a height of only 2 cm. The finger motion measurement was achieved by applying the previously developed mechanism with flexible cables and potentiometers.

For force feedback, the motor followed the finger motion with cable slack when no force was required, and the force was applied by feedback control of the motor current. A smooth transition control strategy was exploited to switch between two controllers without any sudden movement of the motor at the boundaries of different control strategies. The prototype of three finger was manufactured with a small weight and volume of 320 g and $13 \times 23 \times 8\,cm^3$, respectively. The control strategy was validated experimentally and implemented to the hand exoskeleton system. Experiments with virtual objects were also carried out to show the effectiveness of the proposed system.

As future works, the proposed device will be integrated with actual VR environment. Also, the performance evaluation by holding the object with the force sensor will be carried out. The quantitative performance in terms of human perception will be evaluated by psychophysical experiments, and subjective evaluation about satisfaction, usability and design of the system will be verified by user experience evaluation. For adaptability to different hand sizes, the proposed system can allow a variety of hand sizes within the range that the glove can be stretched because the finger structures are made independently and are connected by cables. But, the proposed device will be made with different sizes of gloves (e.g., small, medium, and large) to address significantly different hand sizes. Also, hand position and orientation measurement is required for manipulating objects. By implementing inertial measurement unit (IMU) on the dorsum of the hand and camera based motion capture system, hand position and orientation will be measured.

Acknowledgement

This work was supported by the Global Frontier R&D Program on < Human-centered Interaction for Coexistence > funded bythe National Research Foundation of Korea grant funded bythe Korean Government(MSIP) (NRF-2012M3A6A3056354)

References

[1] Amis AA. Variation of finger forces in maximal isometric grasp tests on a range of cylinder diameters. J Biomed Eng 1987;9(4):313–20.
[2] Basdogan C. Force-reflecting deformable objects for virtual environments. Haptics: From Basic Principles to Advanced Applications. 1999. p. 8–13.
[3] Buja GS, Menis R, Valla MI. Disturbance torque estimation in a sensorless dc drive. Proceedings of the IEEE International Conference on Industrial Electronics, Control, and Instrumentation (IECON). 1993. p. 977–82.
[4] Chiri A, Vitiello N, Giovacchini F, Roccella S, Vecchi F, Carrozza MC. Mechatronic design and characterization of the index finger module of a hand exoskeleton for post-stroke rehabilitation. IEEE/ASME Trans Mechatron 2012;17:884–94.
[5] CyberGlove Systems. Cybergrasp. 2017. http://www.cyberglovesystems.com/.
[6] Force dimension. Omega.3. 2017. http://www.forcedimension.com/.
[7] Frisoli A, Simoncini F, Bergamasco M, Salsedo F. Kinematic design of a two contact points haptic interface for the thumb and index fingers of the hand. J Mech Des

2007;129(5):520–9.
[8] Geomagic. Geomagic touch x. 2017. http://www.geomagic.com/.
[9] Google VR. Cardboard. 2017. https://vr.google.com/.
[10] Heo P, Gu GM, jin Lee S, Rhee K, Kim J. Current hand exoskeleton technologies for reahabilitation and assistive engineering. Int J Precis Eng Manuf 2012;13.5:807–24.
[11] Ho N, Tong K, Hu X, Fung K, Wei X, Rong W, et al. An emg-driven exoskeleton hand robotic training device on chronic stroke subjects. Proc. the IEEE International Conference on Rehabilitation Robotics (ICORR). 2011. p. 1–5.
[12] HTC Corporation. Vive controller. 2017. https://www.vive.com/.
[13] Hume MC, Gellman H, McKellop H, Brumfield RH. Functional range of motion of the joints of the hand. J Hand Surg Am 1990;15.2:240–3.
[14] Iqbal J, Ahmad O, Malik A. HEXOSYS II-towards realization of light mass robotics for the hand. IEEE International Multitopic Conference(INMIC). 2011. p. 115–9.
[15] Jeong D, Jo I, Bae J. Analysis on the force distribution of various grasps for the design of a hand exoskeleton. Proc. the IEEE International Conference on Ubiquitous Robots and Ambient Intelligence(URAI). 2014. p. 127–31.
[16] Kang BB, Lee H, In H, Jeong U, Chung J, Cho K-J. Development of a polymer-based tendon-driven wearable robotic hand. IEEE International Conference on Robotics and Automation (ICRA). 2016. p. 3750–5.
[17] Kim KH, Nam YJ, Park RYMK. Smart mouse: 5-dof haptic hand master using magneto-rheological fluid actuators. J Phys Conf Ser 2009;149:012062.
[18] Koyama T, Yamano I, Takemura K, Maeno T. Multi-fingered exoskeleton haptic device using passive force feedback for dexterous tele-operation. IEEE/RSJ International Conference on Intelligent Robots and Systems. 3. 2002. p. 2905–10.
[19] Kunesch E, F.Binkofski, Freund H. Invariant temporal characteristics of manipulative hand movements. Exp Brain Res 1989;78.3:539–46.
[20] Leijnse J, Quesada P, C.W.Spoor. Kinematic evaluation of the fingers interphalangeal joints coupling mechanism-variability, flexion-extension differences, triggers, locking swanneck deformities, anthropometric correlations. J Biomechatron 2010;43:2381–93.
[21] Marco F, Salsedo Fabio SM, Bergamasco M. Haptic hand exoskeleton for precision grasp simulation. J Mech Robot 2013;5.
[22] Maxon motor. Dcx 16 series. 2017. https://www.maxonmotor.com/.
[23] Neumann DA. Kinesiology of the musculoskeletal system : foundations for rehabilitation. Elsevier Health Sciences.; 2013.
[24] Oculus. Oculus lift. 2017. https://www.oculus.com/.
[25] Park Y, Lee J, Bae J. Development of a wearable sensing glove for measuring the motion of fingers using linear potentiometers and flexible wires. IEEE Trans Industr Inform (TII) 2015;11:198–206.
[26] Ponce J, Faverjon B. On computing three-finger force-closure grasps of polygonal objects. IEEE Trans Robotics and Autom 1995;11.6:868–81.
[27] Redmond B, Aina R, Gorti T, Hannaford B. Haptic characteristics of some activities of daily living. IEEE Haptics Symposium. 2010. p. 71–6.
[28] Rice MS, Leonard C, Carter M. Grip strengths and required forces in accessing everyday containers in a normal population. Am J Occupat Therapy 1998;52(8):621–6.
[29] Richard C, Cutkosky MR. Contact force perception with an ungrounded haptic interface. the ASME Dynamic Systems and Control Division. 1997. p. 187–93.
[30] Rijpkema H, Girard M. Computer animation of knowledge-based human grasping. ACM Siggraph Comput Graph 1991;25:339–48.
[31] Tadano K, Akai M, Kadota K, Kawashima K. Development of grip amplified glove using bi-articular mechanism with pneumatic artificial rubber muscle. In Proc. the IEEE International Conference on Robotics and Automation. 2010. p. 2363–8.
[32] Tan HZ, Srinivasan MA, Eberman B, Cheng B. Human factors for the design of force-reflecting hatpic interfaces. Dynamic Systems and Control 1994;55.1:353–9.

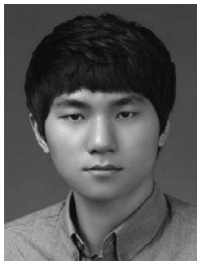

Yeongyu Park received the B.S. degree in mechanical and advanced materials engineering from the Ulsan National Institute of Science and Technology (UNIST), Ulsan, Korea, in 2014. Since 2014, he has been working toward the Ph.D. degree in mechanical engineering at UNIST. His current research interests include wearable hand exoskeleton systems and human – machine Interaction systems.

Inseong Jo received the B.S. degree in mechanical and advanced materials engineering from the Ulsan National Institute of Science and Technology (UNIST), Ulsan, Korea, in 2013. Since 2013, she has been working toward the Ph.D. degree in mechanical engineering at UNIST. Her current research interests include virtual reality and rehabilitation system.

Jeongsoo Lee received the B.S. degree in mechanical and advanced materials engineering from the Ulsan National Institute of Science and Technology (UNIST), Ulsan, Korea, in 2014. Since 2014, he has been working toward the Ph.D. degree in mechanical engineering at UNIST. His current research interests include wearable hand exoskeleton systems, rehabilitation systems.

Joonbum Bae received the B.S. degree in mechanical and aerospace engineering (summa cum laude) from Seoul National University, Seoul, South Korea, in 2006, and the M.S. degree in mechanical engineering, the M.A. degree in statistics, and the Ph.D. degree in mechanical engineering from the University of California at Berkeley, Berkeley, CA, USA, in 2003, 2010, and 2011, respectively.

In 2012, he joined the Department of Mechanical Engineering, Ulsan National Institute of Science and Technology (UNIST), Ulsan, South Korea, where he is currently the Director of the Bio-Robotics and Control Laboratory. His current research interests include modeling, design, and control of human-robot interaction systems, soft robotics, and biologically inspired robot systems.

Dr. Bae received the Korean Government Minister Awards from 'Ministry of Public Safety and Security' and 'Ministry of Science, ICT and Future Planning' in 2016 and 2017, respectively. He also received the Young Researcher Award from the Korea Robotics Society (KROS) in 2015. He was a finalist of the Semi-Plenary Paper Award at the American Society of Mechanical Engineers (ASME) Dynamic Systems and Control Conference in 2012, and a finalist of the Best Poster Paper Award at the International Federation of Automatic Control (IFAC) World Congress in 2008. He received a Samsung Scholarship during the Ph.D. studies.